

## Novel Layered Superstructures in Mixed Ultralong $n$ -Alkanes

X. B. Zeng and G. Ungar\*

*Department of Engineering Materials, University of Sheffield, Sheffield S1 3JD, United Kingdom*

(Received 23 November 2000)

Two new types of layered structures were found in binary mixtures of  $n$ -alkanes ranging from  $C_{122}H_{246}$  to  $C_{294}H_{590}$ . At high temperatures a semicrystalline form is the stable phase, having a regular structure of alternating crystalline and amorphous layers. The two long-chain compounds are mixed in the crystalline layers and the amorphous layers consist of the surplus length of the longer chains. At lower temperatures a reversible transition occurs to a triple layer superlattice structure with a periodicity of up to 50 nm. These two new phases allow the existence of binary solid solutions of chains with a length ratio of up to 1.7 and a chain length difference of 100  $CH_2$  groups.

DOI: 10.1103/PhysRevLett.86.4875

PACS numbers: 68.65.Cd, 61.10.Eq, 61.41.+e, 61.66.Hq

Linear alkanes ( $n$ - $C_nH_{2n+2}$ ) crystallize as extended chains arranged in layers [1]. Those longer than 120 carbon atoms can also crystallize as folded chains [2,3], making them ideal models for the study of polymers where chain-folded crystallization predominates [4]. Pure very long alkanes show some remarkable crystallization phenomena [5], revealing details of the mechanism of polymer crystallization. Our current studies of binary mixtures aim to bridge the gap between the pure model compounds and the real polydisperse polymers.

It has been thought that binary mixtures of short alkanes do not form solid solutions unless the chain lengths differ by less than 3 to 4 carbon atoms [6,7]. In these cases conformational disorder due to mixing is confined to chain ends [8]. More recently new modes of cocrystallization have been suggested for mixtures of alkanes which differ by 4 to 10 C atoms [9–13]. Although ultralong paraffins, up to  $C_{390}H_{782}$ , were first synthesized in 1985 [3,14], it was only recently that a sufficiently wide range was produced [15] to allow a study of their mixtures. We now show how crystalline layered superlattices with periodicities of several hundred angstroms can be produced by self-assembly of long-chain molecules. We also describe binary alkanes with chain lengths differing by up to 100 C atoms displaying molecular miscibility and a stable semicrystalline phase.

Figure 1 shows a series of small-angle x-ray scattering (SAXS) curves recorded during heating of a 1:1 w:w mixture of  $n$ -alkanes  $C_{162}H_{326}$  and  $C_{246}H_{494}$ . A series of Bragg diffraction peaks arise from regular stacking of molecular layers. A clear transition occurs at around 105 °C with melting at 130 °C. Wide-angle scattering (WAXS) shows the crystal unit cell to be that of polyethylene [16], remaining unchanged in the transition. An identical but temperature-shifted reverse series of diffractograms is obtained on cooling the sample from the melt at 2 °C  $min^{-1}$ ; the temperature of both transitions is lowered by 10 °C [17]. Similar behavior is observed in a wide range of compositions, as well as in other binary mixtures involving alkanes  $C_{122}H_{246}$ ,  $C_{162}H_{326}$ ,  $C_{194}H_{390}$ ,  $C_{210}H_{422}$ ,  $C_{246}H_{494}$ ,  $C_{258}H_{518}$ , and  $C_{294}H_{590}$ .

The SAXS traces above 110 °C in Fig. 1 show a single periodicity  $L = 215$  Å, which is between the values for extended-chain  $C_{162}H_{326}$  (170 Å) and  $C_{246}H_{494}$  (258 Å) [2]. Hence the two alkanes are not segregated in isolated lamellar stacks. The large number of diffraction orders and the sharpness of the peaks mean that the layers are of uniform thickness and that the stacking order is good. Thus the structure is also not of the type reported for blends of  $C_{30}H_{62} + C_{36}H_{74}$  [9], where the two paraffins segregate into separate layers but the layers pack in randomly mixed stacks. From the corrected intensities  $I_n$  of the diffraction orders  $n$  we have reconstructed the differential one-dimensional electron density profiles  $\Delta\eta_{exp}(x)$  along the layer normal, using [18]

$$\Delta\eta_{exp}(x) \approx \sum_{n=1}^N \sqrt{I_n} \cos(q_n x + \phi), \quad \phi = 0, \pi.$$

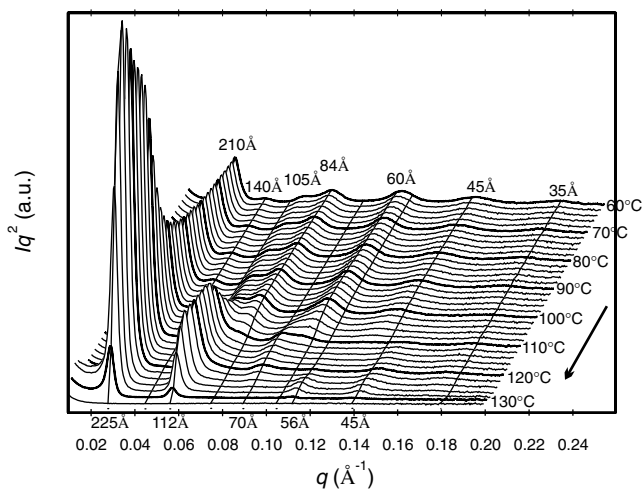


FIG. 1. Series of SAXS traces of a 1:1 w:w mixture of  $C_{162}H_{326}$  and  $C_{246}H_{494}$ , cooled from melt at 2 °C  $min^{-1}$  and recorded during heating at 5 °C  $min^{-1}$ . Constant  $q$  lines are labeled by the corresponding Bragg spacings (in Å). The experiment was done at the Synchrotron Radiation Source at Daresbury, U.K. The mixture was prepared by weighing the alkanes in a glass test tube and melting repeatedly under nitrogen.

Here  $\Delta\eta(x) = \eta(x) - \langle\eta\rangle$ , where  $\eta(x)$  and  $\langle\eta\rangle$  are local and average electron densities,  $q$  is the wave vector, and  $N$  is the number of diffraction orders analyzed. The resulting “experimental” profile  $\Delta\eta_{\text{exp}}(x)$  is shown in Fig. 2 as dots. Superimposed is the profile  $\Delta\eta_N(x)$  calculated from the best-fit trapezoidal model  $\Delta\eta_{\infty}(x)$  using the same number ( $N$ ) of Fourier terms as in  $\Delta\eta_{\text{exp}}(x)$ :

$$\Delta\eta_N(x) = \sum_{n=1}^N A_n \cos\left(\frac{2\pi nx}{L}\right),$$

where

$$A_n = \frac{2}{L} \int_0^L \Delta\eta_{\infty}(x) \cos\left(\frac{2\pi nx}{L}\right) dx.$$

Figure 2 also displays the model  $\Delta\eta_{\infty}(x)$ . The good agreement between  $\Delta\eta_{\text{exp}}(x)$  and  $\Delta\eta_N(x)$  shows that the real density profile is best described by a model  $\Delta\eta_{\infty}(x)$  consisting of a high- and a low-density phase separated by a transition layer with a density gradient. The fit between  $\Delta\eta_{\text{exp}}(x)$  and  $\Delta\eta_N(x)$  is only marginally poorer if a simpler rectangular model is assumed consisting only of a high- and a low-density layer of respective thicknesses  $\ell_c$  and  $\ell_a$ . Figure 3 shows SAXS curves of the high-temperature phase of several binary blends of  $\text{C}_{162}\text{H}_{326}$  with alkanes ranging from  $\text{C}_{194}\text{H}_{390}$  to  $\text{C}_{258}\text{H}_{518}$ ; the trace for pure  $\text{C}_{162}\text{H}_{326}$  is also included. The corresponding best-fit rectangular  $\Delta\eta_{\infty}(x)$  profiles are shown in the inset. In all cases  $\ell_c$  is  $155 \pm 2$  Å. At the same time  $\ell_a$

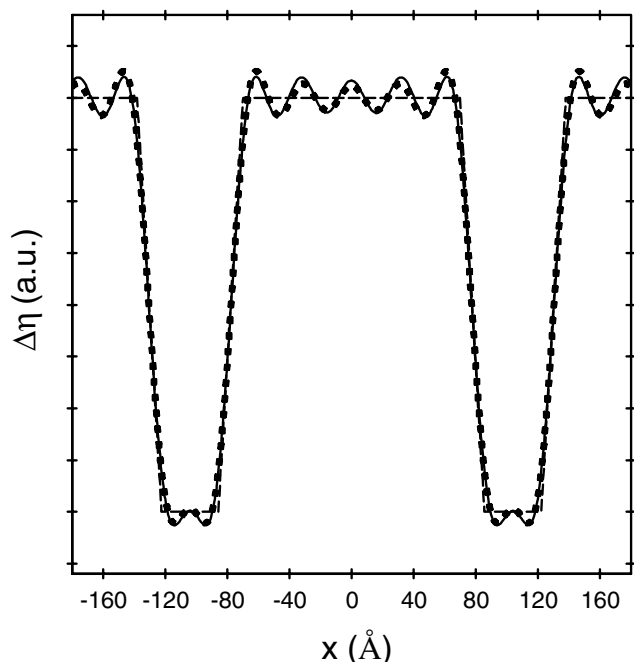


FIG. 2. Electron density profiles normal to the layers of the high-temperature phase:  $\Delta\eta_{\text{exp}}(x)$  using the phase sign sequence  $+-+-+$  (dots), best fit model  $\Delta\eta_{\infty}(x)$  (straight lines), and  $\Delta\eta_N(x)$  calculated from  $\Delta\eta_{\infty}(x)$  using  $N = 6$  Fourier terms (wavy line). The good agreement between  $\Delta\eta_{\text{exp}}(x)$  and  $\Delta\eta_N(x)$  means that the ripples are artifacts of truncation.

increases with increasing length of the longer alkane, from 14 Å for pure  $\text{C}_{162}\text{H}_{326}$  and 37 Å for  $\text{C}_{194}\text{H}_{390}$  to 83 Å for  $\text{C}_{258}\text{H}_{518}$ . The proposed structure of the high-temperature phase is therefore one of alternating crystalline and amorphous layers (Fig. 4A). The crystalline layers contain extended chains of the shorter alkane and crystalline portions of the longer alkane. The amorphous layers contain the surplus length of the longer alkane chains protruding from the crystals as loose *cilia*. The measured heat of fusion of SCF in the 1:1  $\text{C}_{162}\text{H}_{326} + \text{C}_{246}\text{H}_{494}$  mixture (236 J/g) gives a crystallinity of 81%, or 78% by volume, in good agreement with the volume crystallinity  $\ell_c/(\ell_c + \ell_a) = 75\%$  from SAXS. The corresponding WAXS crystallinity was 79%.

As expected,  $\ell_a$  increases with increasing surplus length (Fig. 3), as well as with increasing proportion of the longer alkane in the mixture [17]. The semicrystalline form (SCF) is found in a broad range of compositions with molar fraction of the shorter alkane between  $\approx 0.5$  and 1.

The high-temperature phase in binary long alkanes is unique in that it is a thermodynamically stable semicrystalline phase made up of fully crystallizable chains. The liquidlike and the crystalline layers are integral parts of the phase. Alternating crystalline-amorphous layer structures are common in semicrystalline polymers [4], but they are metastable and are the result of crystallization kinetics. Compared to the phase-separated extended-chain crystal state, in the mixed SCF of the  $\text{C}_{162}\text{H}_{326} + \text{C}_{246}\text{H}_{494}$  1:1 w:w sample the free energy at 390 K is higher by  $\Delta F_c = x(n_\ell - n_s)(T^0 - T)\Delta S = 8.2 \text{ kJ} \cdot \text{mol}^{-1}$  due to uncrystallized cilia, where  $n_\ell - n_s$  is the difference in alkane carbon numbers,  $x$  the molar fraction

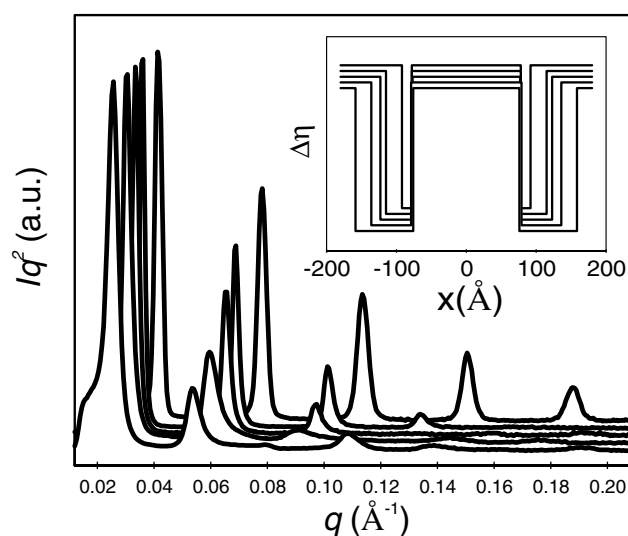


FIG. 3. Small-angle diffractograms of  $\text{C}_{162}\text{H}_{326}$  and of the high-temperature phase of 1:1 w:w binary mixtures of  $\text{C}_{162}\text{H}_{326}$  with, from top to bottom,  $\text{C}_{194}\text{H}_{390}$ ,  $\text{C}_{210}\text{H}_{422}$ ,  $\text{C}_{246}\text{H}_{494}$ , and  $\text{C}_{258}\text{H}_{518}$ . The inset shows the corresponding best-fitting electron density profiles. The total thickness  $\ell_c + \ell_a$  for pure  $\text{C}_{162}\text{H}_{326}$  is 170 Å, which is in agreement with extended chains tilted by  $35^\circ$  to the normal of a layer with  $\{201\}$  basal planes [2].

of longer alkane,  $T^0$  the equilibrium melting point of polyethylene (415 K [19]), and  $\Delta S$  the entropy of fusion. At the same time the free energy is reduced by the entropy of mixing ( $-T \Delta S_{\text{mix}} = -2.2 \text{ kJ} \cdot \text{mol}^{-1}$ ) and the translational unfreezing of the longer molecules [ $-xRT \ln(n_\ell - n_s) = -5.5 \text{ kJ} \cdot \text{mol}^{-1}$ ]. We suggest that the small remaining surplus of  $0.5 \text{ kJ} \cdot \text{mol}^{-1}$  is easily compensated for in SCF through the lowering of end-surface free energy relative to that for extended chain crystals ( $12 \text{ kJ} \cdot \text{mol}^{-1}$ ), as SCF allows surface roughness without chain-end overcrowding.

A related phase has been observed in pure ultralong alkanes [20]. This “noninteger” form (NIF) is also semicrystalline and can be regarded as a mixture of folded and nonfolded chains. However, NIF is transient and transforms within minutes to the fully crystalline extended-chain form [21]. This behavior of NIF supports the argument that molecular mobility in SCF is adequate and that failure to demix during prolonged annealing is evidence of its thermodynamic stability.

Below  $105^\circ\text{C}$  (Fig. 1) the diffractograms are considerably more complex. Curve resolution reveals peaks corresponding to the 2nd, 3rd, 4th, 5th, 7th, 9th, 10th, and 12th orders of a  $L = 420 \text{ \AA}$  periodicity. This  $L$  is close to the sum of extended chain lengths of  $\text{C}_{162}\text{H}_{326}$  and  $\text{C}_{246}\text{H}_{494}$  tilted at the usual angle of  $35^\circ$  ( $428 \text{ \AA}$ ). Experimental intensities agree well with an electron density model  $\Delta\eta_\infty(x)$  shown on the right in Fig. 4B. One full period contains one deep dip in  $\Delta\eta$  and two shallow ones of half the depth.  $\ell_e$ ,  $\ell_m$ ,  $\ell_{s1}$ , and  $\ell_{s2}$  were independent fitting parameters, with  $2\ell_e + \ell_m + \ell_{s1} + 2\ell_{s2} = L$ . Measured and calculated intensities are compared in Fig. 5 for mixtures of  $\text{C}_{162}\text{H}_{326}$  with three longer alkanes:  $\text{C}_{210}\text{H}_{422}$ ,  $\text{C}_{246}\text{H}_{494}$ , and  $\text{C}_{258}\text{H}_{518}$ . The best-fit  $\Delta\eta_\infty(x)$  models A'–C' show that the main effect of increasing the length of the longer alkane is to increase  $\ell_m$ ; at the same time  $\ell_e$  remains constant and equal to  $\ell_c$  in the SCF or in the extended-chain form in pure  $\text{C}_{162}\text{H}_{326}$ .

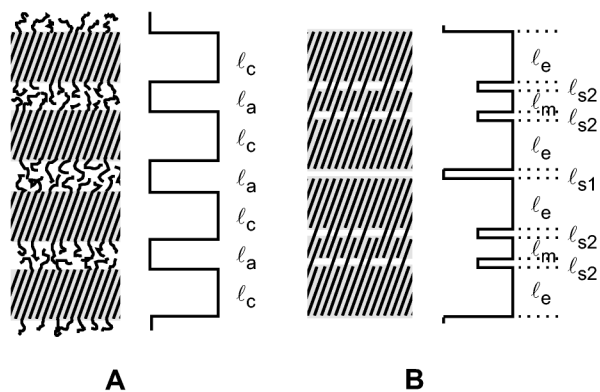


FIG. 4. Schematic structures of (A) the high-temperature semicrystalline phase, and (B) the low-temperature triple-layer superlattice. Model electron density profiles are shown on the right, with  $\eta$  increasing from left to right.

We thus propose a triple-layer superlattice model for the low-temperature phase (Fig. 4B). The two outer layers  $\ell_e$  contain extended chains of the shorter alkane ( $\text{C}_{162}\text{H}_{326}$ ) as well as the major portion of the longer chain molecules. The middle layer  $\ell_m$  contains only the surplus length of the longer molecules protruding from the two end layers. All three layers are crystalline, although there is evidence from WAXS and calorimetry [22] that crystal perfection of the middle layer is poor. The SCF  $\rightarrow$  superlattice transition must occur through pairs of SCF layers acting in tandem.

Additional confirmation of the triple-layer structure is provided by Raman scattering, where the frequency of the first longitudinal acoustic mode (LAM-1) is inversely related to the length of the straight all-trans portion of a polymethylene chain [23]. LAM spectra with increasing temperature are shown in Fig. 6. At low temperatures the two LAM-1 peaks correspond to 165 and 85 carbon all-trans chains [24], i.e., to the lengths of chains traversing, respectively, the outer and the middle layers of the superlattice structure. There is no LAM peak around  $10 \text{ cm}^{-1}$  which would indicate extended chains of  $\text{C}_{246}\text{H}_{494}$ . This

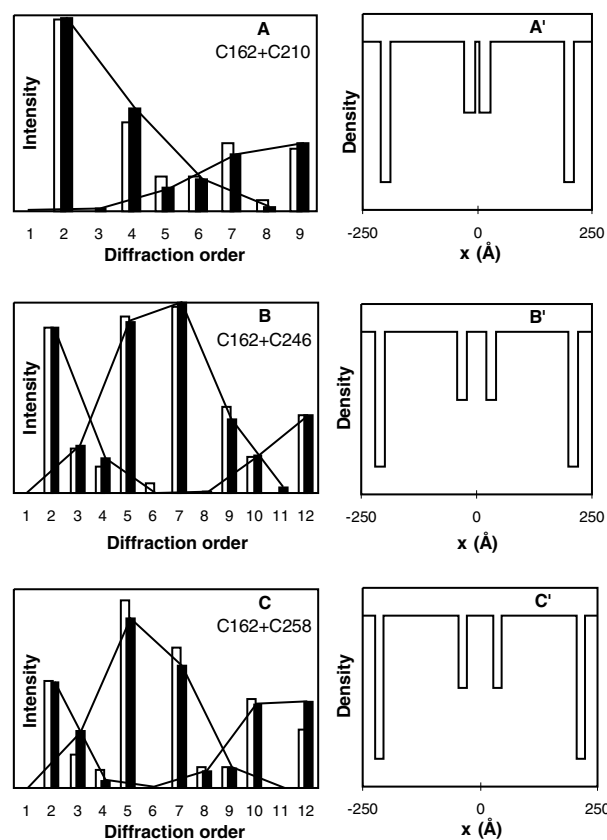


FIG. 5. (A), (B), (C) Diffraction intensities of the triple-layer low-temperature phase of 1:1 w:w alkane mixtures: experimental ( $\square$ ) and calculated ( $\blacksquare$ ) using the model electron density profiles (A'), (B'), and (C'). (A, A')  $\text{C}_{162}\text{H}_{326} + \text{C}_{210}\text{H}_{422}$  ( $\ell_e = 159 \text{ \AA}$ ,  $\ell_m = 10 \text{ \AA}$ ,  $\ell_{s1} = 22 \text{ \AA}$ ,  $\ell_{s2} = 25 \text{ \AA}$ ); (B, B'):  $\text{C}_{162}\text{H}_{326} + \text{C}_{246}\text{H}_{494}$  ( $\ell_e = 157 \text{ \AA}$ ,  $\ell_m = 45 \text{ \AA}$ ,  $\ell_{s1} = 19 \text{ \AA}$ ,  $\ell_{s2} = 19 \text{ \AA}$ ); (C, C'):  $\text{C}_{162}\text{H}_{326} + \text{C}_{258}\text{H}_{518}$  ( $\ell_e = 160 \text{ \AA}$ ,  $\ell_m = 57 \text{ \AA}$ ,  $\ell_{s1} = 17 \text{ \AA}$ ,  $\ell_{s2} = 18 \text{ \AA}$ ). The intensities of even and odd orders are joined separately.

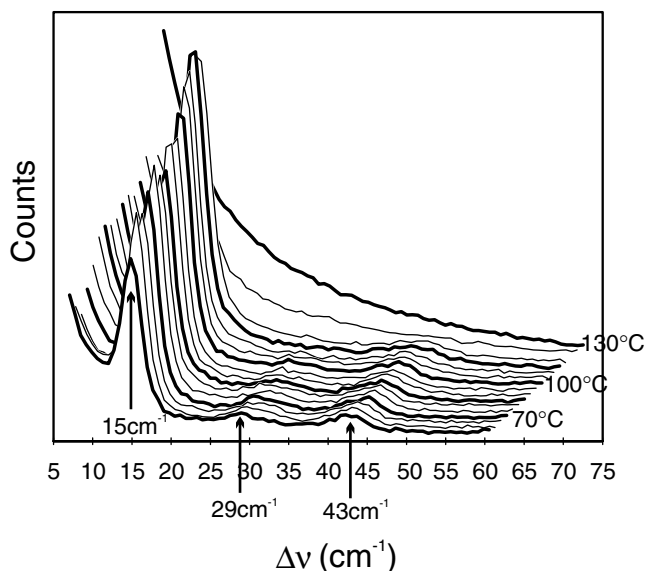


FIG. 6. Series of low-frequency-shift Raman spectra of  $C_{162}H_{326} + C_{246}H_{494}$  (1:1 w:w) with increasing temperature. The peaks at 15, 29, and  $43\text{ cm}^{-1}$  are LAM-1, LAM-1, and LAM-3 modes.

means that the vibrations of the two parts of the  $C_{246}H_{494}$  chain are decoupled. The implication is that  $C_{246}H_{494}$  molecules are not clustered in blocks but are intimately mixed with those of  $C_{162}H_{326}$ . With increasing temperature the  $29\text{ cm}^{-1}$  band gradually weakens and disappears completely at the transition to SCF. Only the  $15\text{ cm}^{-1}$  LAM-1 peak remains, consistent with the proposed structure of SCF.

The authors are greatly indebted to Dr. G.M. Brooke of Durham University for the samples of alkanes, Dr. N.A. Tuan of Jobin-Yvon, Paris, for performing the Raman experiments, and A. Gleeson of Daresbury Laboratory for help with SAXS experiments. This work was supported by EPSRC and the Petroleum Research Fund.

\*Email address: g.ungar@sheffield.ac.uk

- [1] A.E. Smith, *J. Chem. Phys.* **21**, 2229 (1953); H.M.M. Shearer and V. Vand, *Acta Crystallogr.* **9**, 379 (1956); W. Pieszek, G.R. Strobl, and K. Malzahn, *Acta Crystallogr. Sect. B* **30**, 1278 (1974).
- [2] G. Ungar *et al.*, *Science* **229**, 386 (1985).
- [3] K.-S. Lee and G. Wegner, *Makromol. Chem. Rapid Commun.* **6**, 203 (1985).
- [4] A. Keller and G. Goldbeck-Wood, in *Comprehensive Polymer Science*, edited by G. Allen (Pergamon, New York, 1996), Second Suppl., p. 241.
- [5] G. Ungar *et al.*, *Phys. Rev. Lett.* **85**, 4397 (2000).
- [6] H. Luth *et al.*, *Mol. Cryst. Liq. Cryst.* **27**, 337 (1974).
- [7] R.R. Matheson, Jr. and P. Smith, *Polymer* **26**, 288 (1985).
- [8] M. Maroncelli, H.L. Strauss, and R.G. Snyder, *J. Phys. Chem.* **89**, 5260 (1985); Y. Kim, H.L. Strauss, and R.G. Snyder, *J. Phys. Chem.* **93**, 485 (1989).
- [9] D.L. Dorset, *Macromolecules* **18**, 2158 (1985); **19**, 2965 (1986); **20**, 2782 (1987); **23**, 623 (1990).
- [10] R.G. Snyder *et al.*, *J. Phys. Chem.* **97**, 7342 (1993); B.K. Annis *et al.*, *J. Phys. Chem.* **100**, 1725 (1996).
- [11] D.L. Dorset and R.G. Snyder, *J. Phys. Chem.* **100**, 9848 (1996); D.L. Dorset, *J. Phys. Chem. B* **101**, 4870 (1997).
- [12] E.P. Gilbert, *Phys. Chem. Chem. Phys.* **1**, 1517 (1999); **1**, 2715 (1999); **1**, 5209 (1999).
- [13] A.R. Gerson and S. C. Nyburg, *Acta Crystallogr. Sect. B* **50**, 252 (1994).
- [14] I. Bidd and M.C. Whiting, *J. Chem. Soc. Chem. Commun.* **1985**, 543 (1985).
- [15] G.M. Brooke *et al.*, *J. Chem. Soc., Perkin Trans. 1* **1996**, 1635 (1996).
- [16] C.W. Bunn, *Trans. Faraday Soc.* **35**, 483 (1939).
- [17] X.B. Zeng and G. Ungar, "Semicrystalline lamellar phase in binary mixtures of very long-chain *n*-alkanes" (to be published).
- [18] A. Guinier, *X-ray Diffraction in Crystals, Imperfect Crystals, and Amorphous Bodies* (Dover, New York, 1994).
- [19] B. Wunderlich and G. Czornyj, *Macromolecules* **10**, 906 (1977).
- [20] X.B. Zeng and G. Ungar, *Polymer* **39**, 4523 (1998).
- [21] G. Ungar and A. Keller, *Polymer* **28**, 1899 (1987).
- [22] X.B. Zeng and G. Ungar, "Triple layer superlattice in binary mixtures of very long *n*-alkanes" (to be published).
- [23] G.R. Strobl, *J. Polym. Sci. Polym. Phys.* **21**, 1357 (1983).
- [24] G. Ungar, in *Interpretation of Fundamental Polymer Science and Technology*, edited by P.J. Lemstra and I.A. Kleintjens (Elsevier Applied Science Publishing, London, 1988), Vol. 2, p. 342.